

Cuff-less Arterial Blood Pressure Waveform Synthesis from Single-site PPG using Transformer & Frequency-domain Learning

Muhammad Ahmad Tahir*, Ahsan Mehmood*, Muhammad Mahboob Ur Rahman*, Muhammad Wasim Nawaz†, Kashif Riaz*, Qammer H. Abbasi‡

* Electrical engineering department, Information Technology University, Lahore 54000, Pakistan

†Electrical engineering department, University of Lahore, Lahore, Pakistan

‡James Watt School of Engineering, University of Glasgow, Glasgow, G12 8QQ, UK

*{msds21039, mahboob.rahman}@itu.edu.pk, ‡Qammer.Abbasi@glasgow.ac.uk

Abstract—We propose two novel purpose-built deep learning (DL) models for synthesis of the arterial blood pressure (ABP) waveform in a cuff-less manner, using a single-site photoplethysmography (PPG) signal. We utilize the public UCI dataset on cuff-less blood pressure (CLBP) estimation to train and evaluate our DL models. Firstly, we implement a transformer model that incorporates positional encoding, multi-head attention, layer normalization, and dropout techniques, and synthesizes the ABP waveform with a mean absolute error (MAE) of 14. Secondly, we implement a frequency-domain (FD) learning approach where we first obtain the discrete cosine transform (DCT) coefficients of the PPG and ABP signals corresponding to two cardiac cycles, and then learn a linear/non-linear (L/NL) regression between them. We learn that the FD L/NL regression model outperforms the transformer model by achieving an MAE of 11.87 and 8.01, for diastolic blood pressure (DBP) and systolic blood pressure (SBP), respectively. Our FD L/NL regression model also fulfills the AAMI criterion of utilizing data from more than 85 subjects, and achieves grade B by the BHS criterion.

Index Terms—PPG, arterial blood pressure, systolic, diastolic, transformer, ridge regression, discrete cosine transform.

I. INTRODUCTION

Hypertension (high blood pressure) and hypotension (low blood pressure) are two common blood pressure (BP) irregularities that are of great clinical significance. According to the World Health Organization (WHO), approximately 1.28 billion people aged 30-79 years suffer from hypertension, with 46% unaware of it and only 42% receiving treatment [1]. Further, hypertension is more prevalent in low and middle income countries [2]. Hypertension (also known as the silent killer) is a major risk factor for a range of cardiovascular diseases, stroke, chronic kidney disease and pre-mature death [3]. Hypertension, if not treated, could elevate both the systolic BP (SBP) and diastolic BP (DBP) from normal range (below 120/below 80) to stage 1 hypertension (130-139/80-89), to stage 2 hypertension (above 140/above 90), to hypertensive crisis (above 180/above 120), leading to health emergency necessitating immediate hospitalization. Hypotension, though

less frequent than hypertension, is also widespread as approximately (10-20)% of people of age over 65 years experience hypotension. Hypotension occurs when blood pressure falls below 90/60, which could lead to dizziness and nausea. Hypotension becomes perilous when BP falls below 60/45, causing blurriness, confusion, coma, or even death [4]. Thus, regular and frequent monitoring of blood pressure by the elderly is of utmost importance for early diagnosis and efficient management of hypertension and hypotension [5].

The existing clinical-grade methods for blood pressure estimation (including ambulatory devices) could be classified into two categories: i) invasive methods, ii) non-invasive but cuff-based methods. Invasive methods are the gold standard methods which measure the centralized aortic blood pressure by inserting catheters in the aorta (main artery near the heart) [6]. Need not to say that this method is painful, prone to infections, and required trained professionals in a clinical setting. Next, non-invasive but cuff-based methods work by inflating the cuff around the arm and rely upon manual auscultation and Sphygmomanometers for peripheral blood pressure estimation. These methods, though highly accurate, suffer from a number of limitations, e.g., inconvenience of regular monitoring, requirement of trained personnel, Sphygmomanometers use toxic mercury, etc [7]–[9]. Further, the need for frequent cuff inflation and deflation makes continuous BP measurement impractical, especially for individuals with weaker arms, or the elderly [10]. Oscillometric devices, though do not require manual auscultation, have relatively lower accuracy as they rely on mean arterial blood pressure (MABP) for estimating both SBP and DBP.

The limitations of the existing invasive methods and cuff-based non-invasive methods have thus prompted the researchers to design novel cuff-less blood pressure (CLBP) estimation methods which are meant to be user-friendly, reliable, and support continuous and at-home BP measurement [7], [11]–[13]. Additionally, advancements in wearable technology (e.g., smart watches, smart bands, fitness trackers, internet of medical things, flexible electronic tattoos, etc.) and assistive gadgets (e.g., smartphones, airpods, etc.) have further accelerated the development of the CLBP estimation methods [14], [15]. CLBP estimation methods either rely upon

This work is supported in part by UK Engineering and Physical Sciences Research Council (EPSRC) under the grants: EP/T021063/1 and EP/T021020/1.

bio-signals such as photoplethysmography (PPG), electrocardiography (ECG), phonocardiography (PCG) acquired non-invasively from one or more body sites [12], or innovative sensor technology, e.g., tonometry [16].

Contributions. Inline with the recent works on CLBP estimation, we propose two novel purpose-built deep learning (DL) models for synthesis of the arterial blood pressure (ABP) waveform in a cuff-less manner, using a single-site PPG signal. We utilize the public UCI dataset on CLBP estimation to train and evaluate our DL models. The main contribution of this work is two-fold:

- We implement a transformer model that incorporates positional encoding, multi-head attention, layer normalization, and dropout techniques, and synthesizes the ABP waveform with a mean absolute error (MAE) of 14.
- We implement a frequency-domain (FD) learning approach where we first obtain the discrete cosine transform (DCT) coefficients of the PPG and ABP signals corresponding to two cardiac cycles, and then learn a linear/non-linear (L/NL) regression between them.

The transformer model (the FD L/NL regression model) achieves an MAE of 19 and 9 (11.87 and 8.01), for diastolic blood pressure (DBP) and systolic blood pressure (SBP), respectively. Our FD L/NL model achieves grade B by the British Hypertension Society (BHS) criterion.

Feasibility. PPG and ABP signals, though of different origins, have a very similar morphology (because both capture the pressure exerted by the blood volume on arterial walls). In other words, the morphology of the two signals is tightly binded to each other, at the sub-cardiac cycle resolution. Furthermore, the recent advances in the generative artificial intelligence (AI) has made it possible to translate one biosignal to another, e.g., [17] translates a PPG signal to an ECG signal, [18] translates a PPG signal to an ABP signal. This motivates us to propose purpose-built DL models for synthesis of the ABP waveform from a single-site PPG waveform.

Outline. Section II provides some necessary background and summarizes selected related work. Section III provides compact details of the public UCI dataset that we have used, and the key data pre-processing steps that we have performed. Section IV describes the two deep learning models we have implemented for cuff-less arterial blood pressure waveform synthesis. Section V presents some selected results. Section VI concludes the paper.

II. BACKGROUND & RELATED WORK

A. Background

Pulse wave analysis methods: During the last decade, researchers have made extensive investigation of the physiological waveforms acquired in a non-invasive manner (e.g., ECG, PPG, PCG, etc.), under the umbrella term of pulse wave analysis (PWA) [12]. The aim of PWA methods is to develop a number of indices to indirectly measure the blood pressure in a cuff-less manner using wearables (e.g., smart watches) and assistive gadgets (e.g., smartphones) [14]. Some prominent indices (markers for blood pressure) include the following: pulse transit time (PTT), pulse arrival time (PAT), and pulse

wave velocity (PWV). Before we delve into the discussion of the related work, it is imperative to formally define the three indices (BP surrogates) as follows:

- PTT is the time taken by a pulse pressure wave to travel from one point of an artery to another. PTT is inversely proportional to the blood pressure. A typical measurement system for PTT includes two PPG sensors placed at two different locations close to the artery [19], [20].
- PAT is the time delay between the R-peak in the ECG signal and the time of arrival of the corresponding (PPG) pulse at the peripheral site, during the same heart beat. In other words, PAT is the time taken by the pulse pressure wave to travel from the heart to the peripheral measurement site. PAT is related to PTT as follows: $PAT = PTT + \text{pre-ejection period}$ [12].
- PWV is the velocity of a pulse pressure wave that travels a distance L from a proximal point to a distal point. PWV is related to PTT as follows: $PWV = \frac{L}{PTT}$ [12].

Despite the good correlation of PTT, PAT and PWV with the blood pressure, these indices have a number of limitations as well, e.g., need for simultaneous and synchronous measurement of two waveforms from two different sites, calibration issues, lack of consensus on translation of PTT/PAT/PWV to BP (i.e., there exist a number of equations to map PTT/PAT/PWV to BP, each with many unknowns that are subject-specific), etc. [21], [12], [19]. *This highlights the need for the design of novel single-site methods for cuff-less blood pressure (CLBP) estimation.*

Regulatory criteria for CLBP estimation methods: Over time, two regulatory bodies have developed standards to grade the performance of the emerging CLBP estimation methods: 1) association for the advancement of medical instrumentation (AAMI), and 2) British hypertension society (BHS)¹.

- The AAMI requires a dataset consisting of at least 85 individuals having low, high, and normal blood pressure. Further, according to AAMI, the mean error (and standard deviation of the error) of a CLBP estimation method should be within 5 mmHg (and 8 mmHg) [23].
- The BHS assigns one of the three letter grades (A, B, C) to each CLBP estimation method. If the model error is less than or equal to 5 mmHg 60% of time, 10 mmHg 85% of time, and 15 mmHg 95% of time, then the model is given grade A. Similarly, if the model error is less than 5 mmHg 50% of time, 10 mmHg 75% of time, and 15 mmHg 90% of time, then the model is given grade B. Finally, if the model error is less than 5 mmHg 40% of time, 10 mmHg 65% of time, and 15 mmHg 85% of time, then the model is given grade C [24].

B. Related work

Since the literature on CLBP estimation is quite vast, we could only summarize selected related works due to space constraints (see [12], [19] and the references therein, which provide a more detailed treatment of the subject). The CLBP

¹Additionally, IEEE has also developed 1708-2014 (and 1708a-2019) standard for wearable cuffless blood pressure measuring devices [22].

estimation methods are mostly PWA methods which are either two-sites/two-waveforms methods or single-site methods. More recently, researchers have extensively used various deep learning (DL) models for ABP waveform synthesis and CLBP estimation.

Single-site-based methods: [25] utilizes single-site PPG data collected from 150 subjects, computes PWV, and feeds it to a learning-based non-parametric regression method in order to estimate MABP, SBP and DBP. [26] collects multi-wavelength, single-site PPG data from 10 subjects, computes the PTT using the IR-PPG and blue-PPG, in order to estimate the DBP and SBP. [27] recruits 22 young healthy subjects to measure their ballistocardiogram (BCG) using the foot-based pressure sensor/force plate, in order to estimate the DBP (SBP) using I-J interval (J-K amplitude) of a BCG. [18] utilizes the UCI dataset and implements the well-known U-Net model to synthesize an ABP waveform from a single PPG waveform.

Two-sites-based methods: [28] proposes a two-sites-based method for CLBP estimation that utilizes a PPG sensor at the fingertip and an impedance plethysmography (IPG) sensor at the wrist in order to compute the PTT which is then translated to SBP and DBP values. [29] recruits 12 young healthy subjects, records their ECG and fingertip PPG data at multiple regular intervals after treadmill exercise, computes the PTT and translates it to the SBP and DBP values. [8] utilizes the ECG and PPG signals from MIMIC-II dataset, pre-processes them, extracts various physiological features, does dimensionality reduction, and implements a number of machine learning regression models to estimate SBP, MABP and DBP. [30] adopts a rather different approach for CLBP estimation whereby authors utilize data from the PPG, pressure, and height sensors (accelerometers), exploiting the fact that movement of the arm changes the natural hydrostatic pressure.

Deep learning-based methods: [31] utilizes the PPG and ABP signals corresponding to 20 subjects from the MIMIC II dataset, and implements a convolutional neural network (CNN) for feature extraction, followed by a long short-term memory (LSTM) network for CLBP prediction. [32] considers 3 subjects from MIMIC II dataset, and utilizes a CNN-LSTM model for ABP waveform synthesis. Paviglianiti et al. [33] utilize both PPG and ECG signals from the MIMIC dataset, and implement a number of DL models, i.e., ResNet, LSTM, WavNet, and more, for CLBP prediction. Brophy et al. [34] utilize PPG signals from the UCI dataset, implement a number of generative adversarial networks (GAN) models in order to realize a federated learning approach for ABP waveform synthesis. They evaluate the performance of their GAN-based federated learning model on a new unseen dataset, the University of Queensland vital signs dataset. Finally, [35] utilizes a CNN, while [36] implements a feedforward neural network for CLBP estimation.

III. THE UCI DATASET & DATA PRE-PROCESSING

A. The UCI public dataset on CLBP estimation

We utilize the cuff-less blood pressure estimation dataset from the University of California Irvine (UCI) machine learning repository [37]. This dataset is basically a subset of (and

pre-processed version of) the MIMIC-II waveform dataset from Physionet databank, which is a large database of electronic health records of the patients from the intensive care unit of the Beth Israel Deaconess Medical Center in Boston, Massachusetts. This UCI dataset contains 12,000 records of (942 patients) that consists of the physiological waveforms carrying information about the vital signs, with length of each record varying between 8 sec and 10 min. Each record is sampled at 125 Hz and contains fingertip PPG, ECG (channel II), and invasive ABP signal (in mmHg). Further, we note that the dataset labels (i.e., DBP and SBP values) lie in the following range: ($60 \leq \text{DBP} \leq 130$) mmHg and ($80 \leq \text{SBP} \leq 180$) mmHg. In this work, we mainly focus on the PPG and ABP waveforms for CLBP estimation.

B. Data Preprocessing

In order to prepare the data for our DL models, we implemented the following data preprocessing steps on the PPG and ABP signals. 1) We began by removing out-of-band noise from the data using a Butterworth low-pass filter with a cut-off frequency of 10 Hz. 2) We then proceeded to remove the residual artifacts manually (by discarding the anomalous samples). 3) Next, we removed the baseline from the data using the Wavelet filtering. 4) We then normalized the data using z-score normalization. 5) Further, the process of ABP waveform synthesis from PPG waveform required beat-level synchronization between the PPG and ABP signals. To this end, we utilized time shifting approach to align the systolic peaks of the PPG signal with the systolic peaks of the ABP signal. 6) We then did segmentation (with a stride of 0) to construct a number of segments from each PPG and ABP recording, in order to increase the size of the dataset. Note that each segment consists of two cardiac cycles.

IV. METHODOLOGY

Keeping in mind that the problem at hand—ABP waveform synthesis from PPG waveform—is a sequence-to-sequence translation (i.e., regression) problem, we have implemented two novel deep learning methods using Tensorflow and Keras frameworks in Python: 1) a transformer model, 2) a linear/non-linear frequency-domain regression model. Once the ABP waveform is synthesized, we sample its maximum and minimum values which yield the systolic and diastolic blood pressure, respectively. Below, we discuss the two methods in detail, one by one.

A. Transformer model for ABP waveform synthesis

The motivation for implementing a transformer model for ABP waveform synthesis from PPG waveform comes from the following: i) both the PPG and the ABP waveforms represent the time-series data, ii) each of the two time-series consists of an ordered set of data points that capture the temporal dynamics of the heart, i.e., the heart physiology, at different time-scales and on its own, iii) there is one-to-one correspondence (relationship) between the (ordered) data points (at the same instant) in the PPG and ABP time-series,

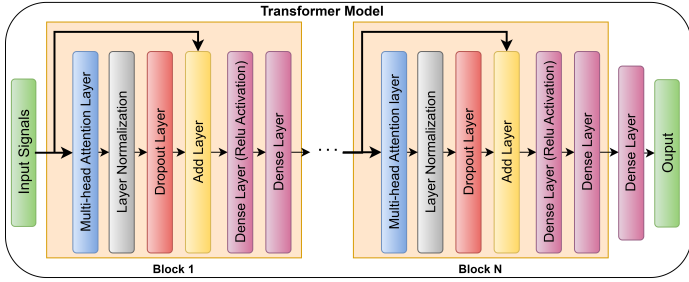


Fig. 1. Architecture of Transformer model for ABP waveform synthesis.

due to the fact that they both capture the same phenomenon (of heart physiology), though independently. Keeping in mind all these strong analogies with the natural language processing (NLP) problems (e.g., language translation, paraphrasing, etc.), we solve the ABP waveform synthesis problem using the transformer model—a powerful tool for solving a range of NLP problems.

Our transformer model implementation consists of the following discrete components: positional encoding, multi-head self-attention, feedforward network, layer normalization, dropout, and a dense output layer. Fig. 1 shows the architecture of the transformer implemented in this work in detail.

At this point, it is imperative to revisit the individual building blocks of the transformer model to see how each component helps solve the problem at hand. 1) First, the positional encoding (often implemented by means of sine and cosine functions) keeps the transformer informed about the order and position of data points (i.e., the notion of time) in each of the two (i.e., PPG and ABP) sequences. 2) Next, the multi-head self-attention mechanism, as the name implies, focuses on capturing relationship between every pair of data points (by means of attention scores) in both the PPG and ABP sequences, using multiple heads that attend to different parts of the PPG and ABP sequences in order to capture the short term and the long term dependencies within the PPG and ABP signals. 3) Next, the layer Normalization reduces the internal covariate shift, prevents the issue of vanishing or exploding gradients, helps prevent overfitting, all by normalizing the activations. 4) The dropout regularization layer randomly sets a fraction of the values to zero during training, which helps to prevent overfitting. 5) Element-wise addition between the original input and the output of the dropout layer is performed in the next block. This residual connection allows information to bypass the self-attention and normalization layers, helping the model retain valuable information from the original input. 6) Next, the feedforward network applies a set of linear transformations and non-linear activations to the input data, allowing the model to learn complex patterns and relationships. 7) Finally, the dense layer produces the output of the model.

B. Linear/non-linear frequency-domain regression model for ABP waveform synthesis

In this method, we follow a two-step approach for ABP waveform synthesis. During the training phase, the two steps

are implemented as follows:

- *Frequency-domain representation of pre-processed data:* Firstly, we obtain the frequency-domain representation of the pre-processed data, for both signals of interest, i.e., PPG and ABP signals. The motivation for this comes from the fact that both PPG and ABP signals are quasi-periodic due to the rhythmic activity of the heart. Specifically, we consider one PPG-ABP segment-pair corresponding to a single cardiac cycle of duration Q' samples, at a time. We then compute the discrete cosine transform (DCT) (type-II) of each of the PPG and ABP segments in the single PPG-ABP segment-pair. Further, it is well-known that the PPG and ABP signals are sparse in frequency domain (with only a few low-frequency components with significant energy). This allows us to have a compact representation of each of the two segments in the given PPG-ABP segment-pair by retaining first Q_X (Q_Y) significant DCT coefficients of the PPG (ABP) segment only. This in turn helps in reducing the computationally complexity of our linear/non-linear (L/NL) regression model by reducing the dimension of the feature vector it takes as input. Note that we zero-pad both DCT vectors of size Q_X and Q_Y to resize them to Q in order to do the L/NL regression in the next step (where Q represents the duration of a cardiac cycle, in samples).
- *Linear/non-linear regression:* Secondly, we learn the linear/non-linear regression between the size- Q DCT coefficients vector \mathbf{x} (that represents the most important features of the PPG signal) and the size- Q DCT coefficients vector \mathbf{y} (that represents the most important features of the ABP signal). For linear regression, we have implemented ridge regression with $\alpha = 0.5^2$. For non-linear regression, we have implemented a shallow feedforward neural network (FFNN) with two hidden layers and a recurrent neural network (RNN) with two hidden layers.

Next, the testing phase. We compute DCT (type-II) of a previously unseen size- Q' PPG segment, resize it to Q_X and then Q . We then feed the size- Q DCT vector (of PPG) to the L/NL frequency-domain regression model which outputs a size- Q DCT vector (of ABP). Then, ABP waveform is synthesized by taking the inverse DCT (I-DCT) of the output of the L/NL regression model. Fig. 2 provides a pictorial overview of the proposed FD L/NL regression model.

V. RESULTS AND DISCUSSION

Performance Metrics: We have utilized the following two metrics to evaluate the performance of our DL models for CLBP estimation: mean absolute error (MAE), and root mean squared error (RMSE), where $\text{MAE} = \frac{1}{N} \sum_{i=1}^N |\hat{y}_i - y_i|$, and $\text{RMSE}(y, \hat{y}) = \sqrt{\frac{\sum_{i=1}^N (y_i - \hat{y}_i)^2}{N}}$. Here, N represents the batch size, y represents the reference value/ground truth, and \hat{y} represents the model prediction.

²Ridge regression is basically linear regression but with an additional term for L_2 regularization that helps prevent overfitting and stabilize the regression coefficients.

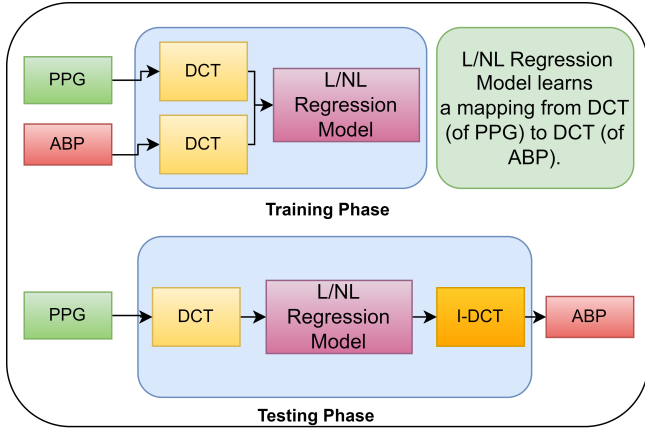


Fig. 2. Architecture of FD L/NL regression model for ABP waveform synthesis.

A. Performance evaluation of Transformer model

Setting of hyperparameters: We used Adam optimizer, and used a learning rate of $1e-3$. Further, we set segment size to 2 seconds, i.e., 250 samples. For training and evaluation of transformer model, we utilized an 80-20 train-test split. In multi-head attention layer, we set number of heads to 8, with the size of each attention head for query and key being 64. Next, the feedforward network consisted of 64 neurons and a relu activation function. The number of transformer layers was varied between 7-15. For layer normalization, we set epsilon to $1e-6$. Finally, we set the dropout ratio to 0.1.

Fig. 3 is a qualitative result that showcases two examples where the transformer model synthesizes the ABP signal from a PPG signal. We make the following observations: 1) It is clear that the morphology of the two synthetic ABP waveforms constructed by the transformer model (on the right) is quite similar to the morphology of the reference ABP waveforms (on the left). 2) We note that the synthetic ABP waveform is shifted in amplitude, compared to the reference ABP waveform. This is the root cause of the error when we measure the SBP and DBP later by sampling the maximum and minimum point of the synthetic ABP waveform.

Now, the quantitative results. The lowest MAE (for ABP waveform synthesis) achieved by the transformer model is 9.10, with 15 layers. That is, the transformer model’s performance increases with increase in number of layers, and reaches a maximum for 15 layers (as further increasing the depth does not result in significant improvements). Further, the transformer model achieved an MAE of 19 and 9, for DBP and SBP, respectively.

B. Performance evaluation of FD L/NL Regression model

Setting of hyperparameters: For ridge regression, we set $\alpha = 0.5$. The rest of the hyperparameters remain the same.

Fig. 4 is again a qualitative result that demonstrates by means of two examples the quality of the ABP signal synthesized by the FD L/NL regression model. It is again evident that the morphology of the two synthetic ABP waveforms produced by the FD L/NL regression model (on the right)

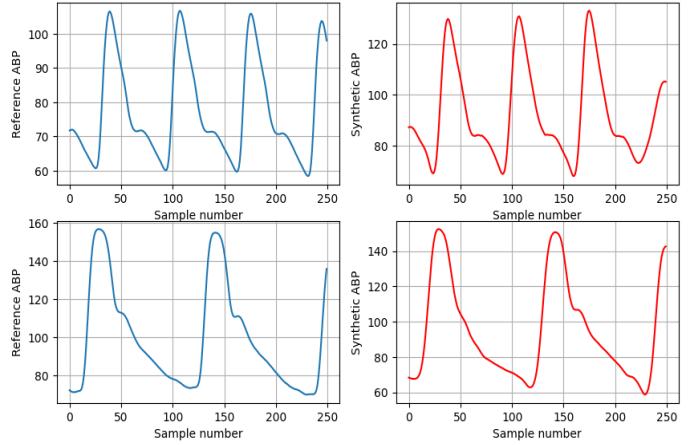


Fig. 3. Two examples of ABP waveform synthesis by our transformer model.

and the morphology of the reference ABP waveforms (on the left) are highly similar. Also, the synthetic ABP waveform is again shifted in amplitude, compared to the reference ABP waveform. But luckily, this time this shift in amplitude of the synthetic ABP is less pronounced. This helps us get a better MAE performance when we measure the SBP and DBP.

For our FD L/NL regression model, after converting the PPG signal to frequency-domain by means of the DCT, we have implemented ridge regression for linear regression purpose, and a feedforward neural network (FFNN) and a recurrent neural network (RNN) for non-linear regression purposes. The resulting MAE performance (for ABP waveform synthesis) is summarized in Table I. We learn from Table I that the ridge regression outperforms the FFNN and RNN by a large margin, which indicates that the relationship between the PPG signal and the ABP signal is perhaps linear.

Finally, our FD L/NL regression model (with ridge regression) achieves an MAE of 8.01 mmHg for DBP and an MAE of 11.87 mmHg for SBP.

TABLE I
PERFORMANCE OF DIFFERENT ARCHITECTURES FOR OUR FD L/NL REGRESSION MODEL

FD L/NL regression model	MAE
DCT + Ridge Regression	8.1
DCT + RNN	17.23
DCT + FFNN	20.24

C. Performance comparison with related work

Table II provides a detailed performance comparison of our work with the selected related works by providing a quick summary of different deep learning models used for CLBP estimation, their corresponding datasets, and the performance achieved by each model. Table II efficiently highlights the variability in the performance of the related works, which is in turn due to the change of data distribution across datasets, variable sizes of the datasets, model architectures, etc. Our first approach, i.e., the transformer based model achieved an MAE of 9.10 for ABP waveform synthesis which is at par with

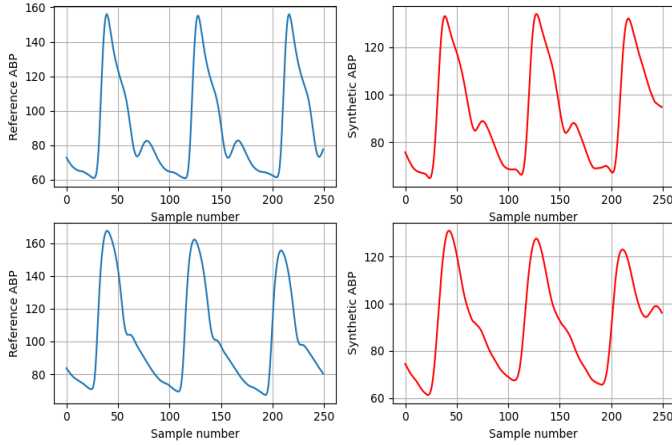


Fig. 4. Two examples of ABP waveform synthesis by our FD L/NL regression model.

the related works. However, the transformer model achieved a relatively large MAE of 19, for DBP estimation, which suggests that our model is well-trained for ABP synthesis and SBP estimation only. Our 2nd approach, i.e., the FD L/NL regression model achieved a MAE of 8.01 for DBP and 11.87 for SBP, which is again at par with the performance reported by the related works.

TABLE II
PERFORMANCE COMPARISON OF OUR WORK WITH THE RELATED WORK: SBP MAE AND DBP MAE ARE IN MMHG. N REPRESENTS NUMBER OF SUBJECTS. * REPRESENTS RMSE IN MMHG.

Work	Dataset	N	Algorithm	SBP	DBP
Tazarv et al. [31]	MIMIC II	20	CNN-LSTM	3.70	2.02
Paviglianiti et al. [33]	MIMIC	40	ResNet, LSTM, WavNet, ResNet+LSTM	4.118	2.228
Treebup-achatsakul et al.	UCI	812	CAN	7.14*	6.08*
Slapnicar et al.	MIMIC III	510	Spectrotemporal ResNet	9.43	6.88
Wang et al.	UCI	348	Pretrained AlexNet, Inception-V3, VGG-19	6.17	3.16
Aguirre et al.	MIMIC	1131	RNN Encoder-Decoder + attention	14.39	14.39
Our work (transformer)	UCI	209	Transformer	19.0	9.0
Our work (FD L/NL regression)	UCI	209	DCT+L/NL Regression	11.87	8.01

Finally, Table III outlines the performance grades of our transformer model and FD L/NL regression model, according to the BHS grading criterion. Specifically, Table III shows the cumulative percentages (CP) of the error achieved by the two models on the UCI test data. We can see that our transformer model achieves the grade C, while our FD L/NL regression model achieves the grade B. For the sake of completeness, Table III also summarizes the BHS performance

TABLE III
PERFORMANCE COMPARISON OF OUR WORK WITH RELATED WORK ACCORDING TO THE BHS CRITERION

Work	Grade	Cumulative Error		
		$\leq 5\%$	$\leq 10\%$	$\leq 15\%$
BHS	A	60%	85%	95%
	B	50	75	90
	C	40	65	85
N. Ibtehaz et. al [18]	A	87.4	95.2	97.7%
Tazarv et. al [31]	A	75	92	96%
Li Y-H et. al	B	59.46	79.97	88.45%
Kauchee et. al [8]	C	44.7	71.6	86.7%
Yang et. al	C	42.1	94.7	100%
Our work (FD L/NL regression)	B	51.69	76.79	100%
Our work (transformer)	C	36.47	71.98	100%

grades obtained by the selected related works, for comparison purposes. We also want to highlight that nearly all the works suffer from the issue of lack of generalization, i.e., as the number of subjects increases, the MAE of the SBP and DBP increases, while the BHS grade tends to fall. On a side note, it is also worth mentioning that both of our models fulfill the AAMI criterion of utilizing more than 85 subjects for training purposes.

VI. CONCLUSION

We evaluated two novel purpose-built DL models on public UCI dataset for CLBP estimation using a single-site PPG signal. The transformer model (the FD L/NL regression model) achieved an MAE of 19 and 9 (11.87 and 8.01), for DBP and SBP, respectively. Our FD L/NL regression model also fulfilled the AAMI criterion of utilizing data from more than 85 subjects, and achieved grade B by the BHS criterion.

Now, some parting thoughts. The UCI dataset consists of data from patients in intensive care units, who are often under the effects of drugs and other medical interventions. Thus, it is difficult to generalize the results of studies—that use the UCI dataset—to other populations, such as healthy adults. Thus, there is a need to evaluate our DL models on larger and diverse datasets in order to increase their generalization capability.

REFERENCES

- [1] World Health Organization, “First who report details devastating impact of hypertension and ways to stop it.” <https://www.who.int/news/item/19-09-2023-first-who-report-details-devastating-impact-of-hypertension-and-ways-to-2023>. Accessed on: Jan. 2, 2024.
- [2] P. Nugroho, H. Andrew, K. Kohar, C. A. Noor, and A. L. Sutrantio, “Comparison between the world health organization (who) and international society of hypertension (ish) guidelines for hypertension,” *Annals of Medicine*, vol. 54, no. 1, pp. 837–845, 2022.
- [3] B. Zhou, P. Perel, G. A. Mensah, and M. Ezzati, “Global epidemiology, health burden and effective interventions for elevated blood pressure and hypertension,” *Nature Reviews Cardiology*, vol. 18, no. 11, pp. 785–802, 2021.
- [4] N. I. Saedon, M. Pin Tan, and J. Frith, “The prevalence of orthostatic hypotension: a systematic review and meta-analysis,” *The Journals of Gerontology: Series A*, vol. 75, no. 1, pp. 117–122, 2020.
- [5] K. L. Tucker, J. P. Sheppard, R. Stevens, H. B. Bosworth, A. Bove, E. P. Bray, K. Earle, J. George, M. Godwin, B. B. Green, *et al.*, “Self-monitoring of blood pressure in hypertension: a systematic review and individual patient data meta-analysis,” *PLoS medicine*, vol. 14, no. 9, p. e1002389, 2017.
- [6] B. Saugel, K. Kouz, A. S. Meidert, L. Schulte-Uentrop, and S. Romagnoli, “How to measure blood pressure using an arterial catheter: a systematic 5-step approach,” *Critical Care*, vol. 24, pp. 1–10, 2020.

- [7] J. A. Pandit, E. Lores, and D. Batlle, "Cuffless blood pressure monitoring: promises and challenges," *Clinical Journal of the American Society of Nephrology: CJASN*, vol. 15, no. 10, p. 1531, 2020.
- [8] M. Kachuee, M. M. Kiani, H. Mohammadzade, and M. Shabany, "Cuffless blood pressure estimation algorithms for continuous health-care monitoring," *IEEE Transactions on Biomedical Engineering*, vol. 64, no. 4, pp. 859–869, 2016.
- [9] P. M. Nabeel, J. Jayaraj, K. Srinivasa, S. Mohanasankar, and M. Chenniappan, "Bi-modal arterial compliance probe for calibration-free cuffless blood pressure estimation," *IEEE Transactions on Biomedical Engineering*, vol. 65, no. 11, pp. 2392–2404, 2018.
- [10] P. Shaltis, A. Reisner, and H. Asada, "A hydrostatic pressure approach to cuffless blood pressure monitoring," in *The 26th Annual International Conference of the IEEE Engineering in Medicine and Biology Society*, vol. 1, pp. 2173–2176, 2004.
- [11] J. A. Pandit, E. Lores, and D. Batlle, "Cuffless blood pressure monitoring," *Clinical Journal of the American Society of Nephrology*, vol. 15, no. 10, p. 1531–1538, 2020.
- [12] J. Solà and R. Delgado-Gonzalo, "The handbook of cuffless blood pressure monitoring," *Cham: Springer*, 2019.
- [13] L.-Y. Shyu, Y.-L. Kao, W.-Y. Tsai, and W. Hu, "Development of a cuffless blood pressure measurement system," in *2012 Annual International Conference of the IEEE Engineering in Medicine and Biology Society*, pp. 2040–2043, 2012.
- [14] H. Y. Lee, D.-J. Lee, J. Seo, S.-H. Ihm, K.-i. Kim, E. J. Cho, H. C. Kim, J. Shin, S. Park, I.-S. Sohn, and et al., "Smartphone / smartwatch-based cuffless blood pressure measurement : A position paper from the Korean society of hypertension," *Clinical Hypertension*, vol. 27, no. 1, 2021.
- [15] J. Baek, J. Kim, N. Kim, D. Lee, and S.-M. Park, "Validation of cuffless blood pressure monitoring using wearable device," in *TENCON 2018 - 2018 IEEE Region 10 Conference*, pp. 0416–0419, 2018.
- [16] M. Park, H. Kang, Y. Huh, and K.-C. Kim, "Cuffless and noninvasive measurement of systolic blood pressure, diastolic blood pressure, mean arterial pressure and pulse pressure using radial artery tonometry pressure sensor with concept of Korean traditional medicine," in *2007 29th Annual International Conference of the IEEE Engineering in Medicine and Biology Society*, pp. 3597–3600, 2007.
- [17] A. Mehmood, A. Sarouji, M. M. U. Rahman, and T. Y. Al-Naffouri, "Your smartphone could act as a pulse-oximeter and as a single-lead ecg," *Scientific Reports*, vol. 13, no. 1, p. 19277, 2023.
- [18] N. Ibtihaz, S. Mahmud, M. E. Chowdhury, A. Khandakar, M. Salman Khan, M. A. Ayari, A. M. Tahir, and M. S. Rahman, "Ppg2abp: Translating photoplethysmogram (ppg) signals to arterial blood pressure (abp) waveforms," *Bioengineering*, vol. 9, no. 11, p. 692, 2022.
- [19] R. Mukkamala, J.-O. Hahn, O. T. Inan, L. K. Mestha, C.-S. Kim, H. Töreyn, and S. Kyal, "Toward ubiquitous blood pressure monitoring via pulse transit time: Theory and practice," *IEEE Transactions on Biomedical Engineering*, vol. 62, no. 8, pp. 1879–1901, 2015.
- [20] R. Shriram, A. Wakankar, N. Daimiwal, and D. Ramdasi, "Continuous cuffless blood pressure monitoring based on ptt," in *2010 International Conference on Bioinformatics and Biomedical Technology*, pp. 51–55, IEEE, 2010.
- [21] K. Shimura, M. Hori, T. Dohi, and H. Takao, "The calibration method for blood pressure pulse wave measurement based on arterial tonometry method," in *2018 40th Annual International Conference of the IEEE Engineering in Medicine and Biology Society (EMBC)*, pp. 1–4, 2018.
- [22] "Ieee standard for wearable cuffless blood pressure measuring devices," *IEEE P1708/D04, June 2014*, pp. 1–32, 2014.
- [23] *Electronic or Automated Sphygmomanometers*. ANSI/AAMI Standard SP10-192, ed. Arlington, VA, USA, 1993.
- [24] E. O'Brien, J. Petrie, W. Littler, M. De Swiet, P. L. Padfield, D. Altman, M. Bland, A. Coats, N. Atkins, et al., "The British Hypertension Society protocol for the evaluation of blood pressure measuring devices," *J Hypertens*, vol. 11, no. Suppl 2, pp. S43–S62, 1993.
- [25] A. Chakraborty, D. Goswami, J. Mukhopadhyay, and S. Chakrabarti, "Measurement of arterial blood pressure through single-site acquisition of photoplethysmograph signal," *IEEE Transactions on Instrumentation and Measurement*, vol. 70, pp. 1–10, 2021.
- [26] J. Liu, Y.-T. Zhang, X.-R. Ding, W.-X. Dai, and N. Zhao, "A preliminary study on multi-wavelength ppg based pulse transit time detection for cuffless blood pressure measurement," in *2016 38th Annual International Conference of the IEEE Engineering in Medicine and Biology Society (EMBC)*, pp. 615–618, 2016.
- [27] C.-S. Kim, A. M. Carek, O. T. Inan, R. Mukkamala, and J.-O. Hahn, "Ballistocardiogram-based approach to cuffless blood pressure monitoring: Proof of concept and potential challenges," *IEEE Transactions on Biomedical Engineering*, vol. 65, no. 11, pp. 2384–2391, 2018.
- [28] T. H. Huynh, R. Jafari, and W.-Y. Chung, "Noninvasive cuffless blood pressure estimation using pulse transit time and impedance plethysmography," *IEEE Transactions on Biomedical Engineering*, vol. 66, no. 4, pp. 967–976, 2019.
- [29] X. F. Teng and Y. T. Zhang, "An evaluation of a ptt-based method for noninvasive and cuffless estimation of arterial blood pressure," in *2006 International Conference of the IEEE Engineering in Medicine and Biology Society*, pp. 6049–6052, 2006.
- [30] P. A. Shaltis, A. T. Reisner, and H. H. Asada, "Cuffless blood pressure monitoring using hydrostatic pressure changes," *IEEE Transactions on Biomedical Engineering*, vol. 55, no. 6, pp. 1775–1777, 2008.
- [31] A. Tazarv and M. Levorato, "A deep learning approach to predict blood pressure from ppg signals," in *2021 43rd Annual International Conference of the IEEE Engineering in Medicine & Biology Society (EMBC)*, pp. 5658–5662, 2021.
- [32] H. Mou and J. Yu, "Cnn-1stm prediction method for blood pressure based on pulse wave," *Electronics*, vol. 10, no. 14, p. 1664, 2021.
- [33] A. Paviglianiti, V. Randazzo, E. Pasero, and A. Vallan, "Noninvasive arterial blood pressure estimation using abpnet and vital-ecg," in *2020 IEEE International Instrumentation and Measurement Technology Conference (I2MTC)*, pp. 1–5, IEEE, 2020.
- [34] E. Brophy, M. De Vos, G. Boylan, and T. Ward, "Estimation of continuous blood pressure from ppg via a federated learning approach," *Sensors*, vol. 21, no. 18, p. 6311, 2021.
- [35] S. Shimazaki, H. Kawanaka, H. Ishikawa, K. Inoue, and K. Oguri, "Cuffless blood pressure estimation from only the waveform of photoplethysmography using cnn," in *2019 41st Annual International Conference of the IEEE Engineering in Medicine and Biology Society (EMBC)*, pp. 5042–5045, 2019.
- [36] U. Senturk, I. Yucedag, and K. Polat, "Cuff-less continuous blood pressure estimation from electrocardiogram(ecg) and photoplethysmography (ppg) signals with artificial neural network," in *2018 26th Signal Processing and Communications Applications Conference (SIU)*, pp. 1–4, 2018.
- [37] M. Kachuee, M. Kiani, H. Mohammadzade, and M. Shabany, "Cuff-Less Blood Pressure Estimation." UCI Machine Learning Repository, 2015. DOI: <https://doi.org/10.24432/C5B602>.